Development of a Beta Function Based Topology Optimization Procedure

David G. Taggart[1], Peter Dewhurst[1], Lucian Dobrot[1] and David D. Gill[2]

[1]University of Rhode Island
College of Engineering
Kingston, RI 02881

[2]Sandia National Laboratories
Albuquerque, NM 87185

Abstract: *A novel finite element based topology optimization scheme has been developed and implemented through the use of Abaqus user subroutines. The procedure is based on an iterative material redistribution scheme in which the desired material distribution at each iteration is imposed. A family of Beta probability density functions is utilized to provide a gradual transition from an initial unimodal material density distribution to a bimodal distribution of fully dense and essentially void regions. The efficiency and validity of the scheme is demonstrated through a number of 2-D and 3-D test cases for which the optimal topology is known from analytic optimality criteria. These test cases include classical minimum weight Michell structures as well as newly derived optimal topologies for 3-D structures.*

To visualize the converged finite element results, procedures are developed to convert the final bimodal material distribution data into contour surfaces of constant density. These contours are then saved in a standardized CAD format (STL) that are imported into commercial CAD software. The CAD models are used directly in rapid manufacturing equipment for the production of prototype parts. Physical prototypes of optimized structures have been manufactured using Laser Engineered Net-Shaping™ (LENS®) and Dimension SST 3D-Printing. In addition to the test cases for which optimal topologies are known from analytic optimality criteria, application of the method to the design of an aerospace component will be presented. The described method is the subject of international patent application number PCT/US2006/062302.

Keywords: Design Optimization, Minimum-Weight Structures, Optimization, Postprocessing.

1. Introduction

Several finite element based optimization schemes have been demonstrated to determine minimum weight structural topologies (1-4). Recent work at the University of Rhode Island (5,6) has led to the development of schemes that can be implemented in Abaqus through the use of user subroutines (7). In this paper, topology optimization using prescribed redistribution is shown to provide a computationally efficient procedure. This scheme provides a robust optimization tool that can be exercised within the Abaqus/CAE user interface.

2. Material Redistribution Scheme

In the topology optimization procedure, the desired final mass of the structure is specified at the beginning of the analysis. This material mass is initially distributed uniformly throughout the design domain resulting in a uniform, partially-dense material. All nodes are assigned an initial relative density $\rho_o = V_f / V_D$, where V_f is the final structural volume and V_D is the volume of the partially-dense design domain. This initial distribution can be described by the probability distribution function, f_o, given by $f_o(\rho) = \delta(\rho - \rho_0)$, where δ is the Dirac delta function and ρ is the relative material density ($0 \leq \rho \leq 1$). The corresponding cumulative distribution function, F_o, is given by $F_o(\rho) = H(\rho - \rho_0)$, where H is the Heaviside step function. The desired final material distribution contains two distinct regions of fully dense material ($\rho = 1$) and regions that have zero relative density (ρ_{min} <<1) with the fully dense regions representing the optimized topology. The final material distribution can be described by the probability distribution function, f_f, given by

$$f_f(\rho) = (1 - \rho_o)\,\delta(\rho - \rho_{\min}) + \rho_o\,\delta(\rho - 1) \quad (1)$$

and the corresponding final cumulative distribution is given by

$$F_f(\rho) = (1 - \rho_o)\,H(\rho - \rho_{\min}) + \rho_o\,H(\rho - 1) \quad (2)$$

A gradual transition from the initial distribution to the final distribution can be achieved through the use of the beta function

$$f(\rho) = \beta(\rho, r, s) = \frac{\rho^{r-1}(1-\rho)^{s-1}}{B(r,s)} \quad (3)$$

where r and s are adjustable parameters and

$$B(r,s) = \frac{\Gamma(r)\,\Gamma(s)}{\Gamma(r+s)} \quad (4)$$

where Γ is the gamma function. The corresponding cumulative distribution function, also known as the incomplete beta function, is given by

$$F(\rho) = \beta_{inc}(\rho, r, s) = \frac{1}{B(r,s)} \int_0^{\rho} (\rho')^{r-1}\,(1-\rho')^{s-1}\,d\rho' \quad (5)$$

A non-dimensional time parameter, t, where $0 \leq t \leq 1$, is introduced and appropriate functions $r(t)$ and $s(t)$ are specified. The functions $r(t)$ and $s(t)$ are selected such that the total mass of material is held constant and a smooth transition from the initial unimodal distribution to the final bimodal distribution is achieved. One such family of distributions are shown in Figures 1 & 2.

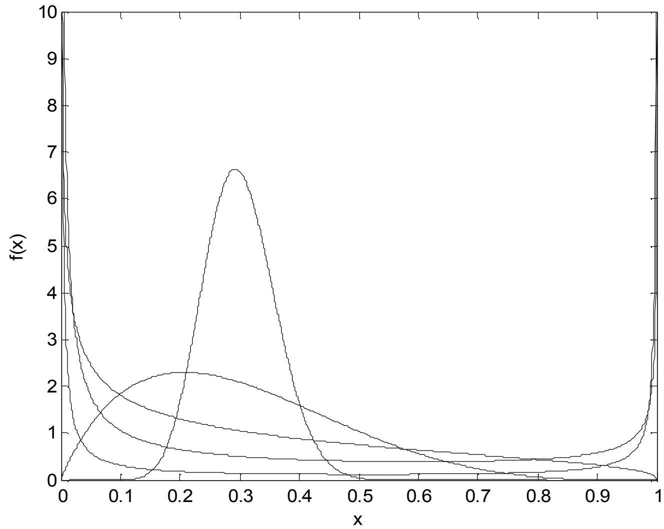

Figure 1. Transition from initial to final distribution for t=0.1, 0.3, 0.5, 0.7 and 0.9.

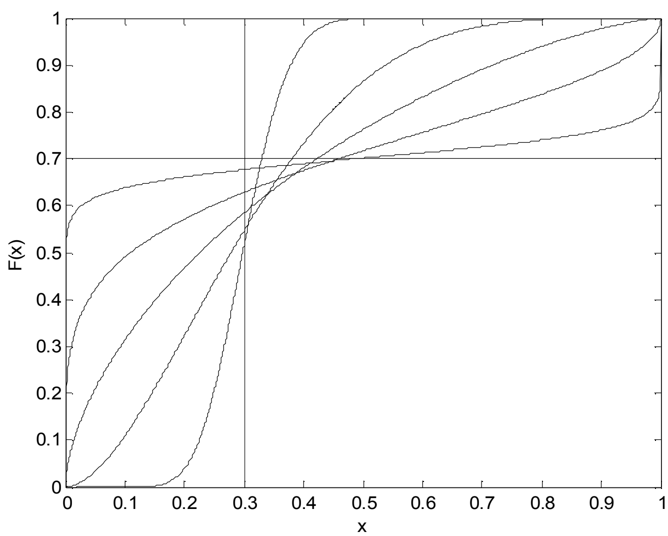

Figure 2. Transition from initial to final cumulative distribution for t=0.0, 0.1, 0.3, 0.5, 0.7, 0.9 and 1.0.

At each finite element iteration, nodal densities are assigned based on the sorted nodal strain energies computed from the previous iteration. Nodes with relatively low strain energy are assigned reduced nodal densities and nodes with relatively high strain energy are assigned increased nodal densities. Through direct assignment of nodal densities, the desired progression of density distributions is enforced. In computing the element stiffness matrices, the nodal density field is interpolated to give the Young's modulus, E, at each Gauss point according to the relation $E = E_d \rho$ where E_d is the fully dense Young's modulus. Convergence to the final topology can be achieved in relatively few finite element iterations.

3. Two dimensional case studies

The 2-D implementation utilizes 4 node quadrilateral elements with full integration. A design domain that extends beyond the expected optimal topology is selected. Four test cases as depicted in Figure 3 are considered. The corresponding optimal topologies for each case are shown in Figure 4. Case 1 is the well known center fan topology first obtained by Michell (8) for the case of a simply supported beam with a single central load and a half-space design domain. Changing the right hand support from a roller to a pin support (Case 2) produces a different topology. This topology, with a mirrored structure about the horizontal axis, is identical to the simply supported beam with a full design domain (Case 3); this solution also appears in Michell's work (8). Case 4 is the well known Chan cantilever (9). All of these results are consistent with topologies obtained through analytic considerations.

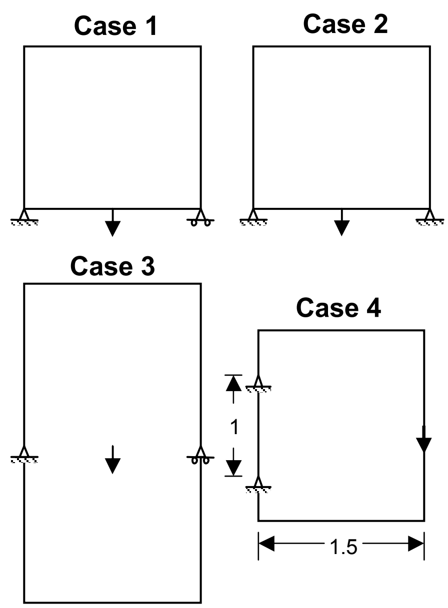

Figure 3. Two Dimensional Test Cases

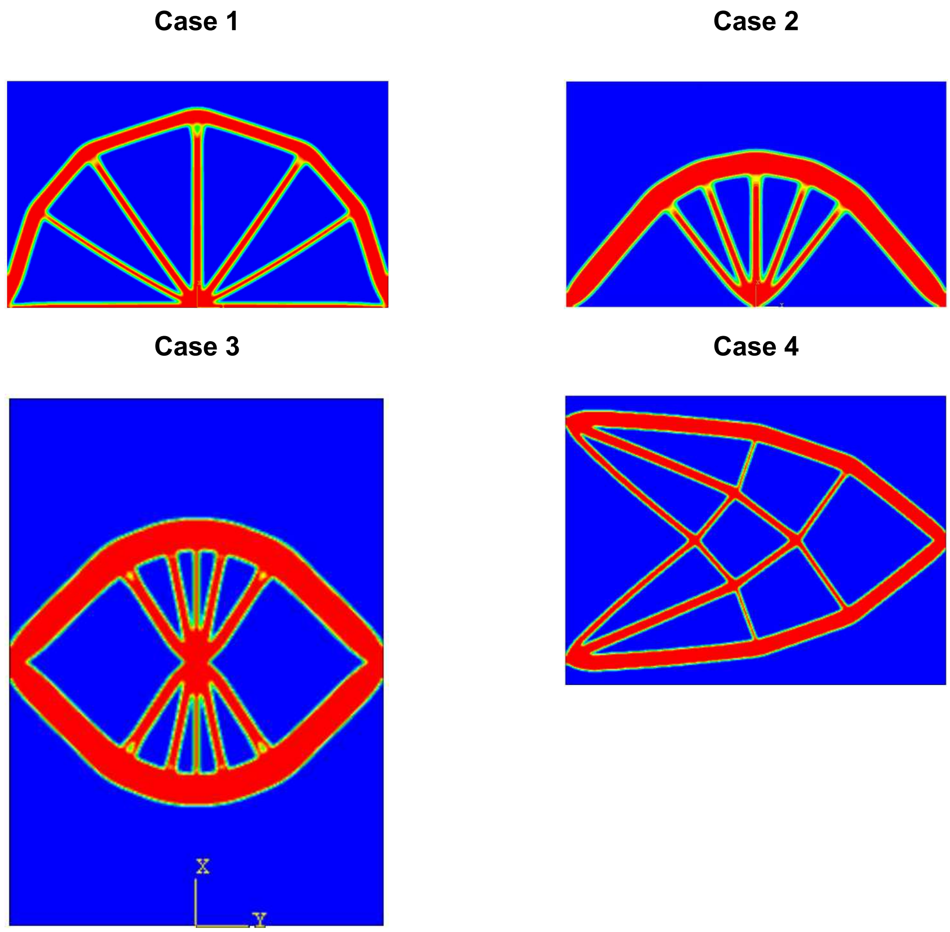

Figure 4. Minimum weight topologies for 2-D test cases

4. Extension to three dimensions

The implementation of the topology optimization scheme in 3-D utilizes 8 node linear hexahedral (brick) elements with full integration. Visualization of the final density field with the Abaqus/CAE environment is achieved using “View Cut” and “Display Group” tools. For improved visualization of the minimum weight topology and for the manufacture of prototype components, a special purpose post-processing code was developed. This code reads model definition and nodal density data from a file created by WRITE statements in the Abaqus user subroutine, URDFIL. The post-processing code reads this data file and, using the marching cube algorithm (10), generates a triangulated surface corresponding to threshold density, typically

ρ=0.5, input by the user. The triangulated surface data is saved in STL format and is available for import to standard CAD software, STL viewers, and rapid manufacturing equipment.

As a demonstration, a 3-D generalization of the 2-D Michell center fan topology (Case 1 above) is investigated. In the 3-D case, the semi-infinite design domain is subjected to a concentrated normal force with equally spaced radial roller supports along a circular region whose center is the load application point. For the case of eight support points, the optimal topology can readily be shown to comprise four Michell 180° arch structures intersecting at the pole. To model this problem, the design domain is taken to be a cylinder whose radius and height exceed the radius to the support locations. Using symmetry, the design domain can be taken as a 1/16 sector of this cylinder (see Figure 5a). An axial concentrated force is applied at the corner point that represents the center of the full cylinder domain. To model each of the 8 support locations, zero axial and circumferential displacement conditions are imposed at a single point along a radial edge of the domain. Finally, symmetry displacement boundary conditions are imposed along the two symmetry planes such that the model represents one sixteenth of the actual full cylinder design domain. The region was meshed using hexahedral elements as shown in Figure 5b.

The optimized topology as represented by the triangulated surfaces generated during post-processing is shown in Figure 6. The results for the 1/16 sector are mirrored to provide the full model topology. Good correlation with the expected topology is observed.

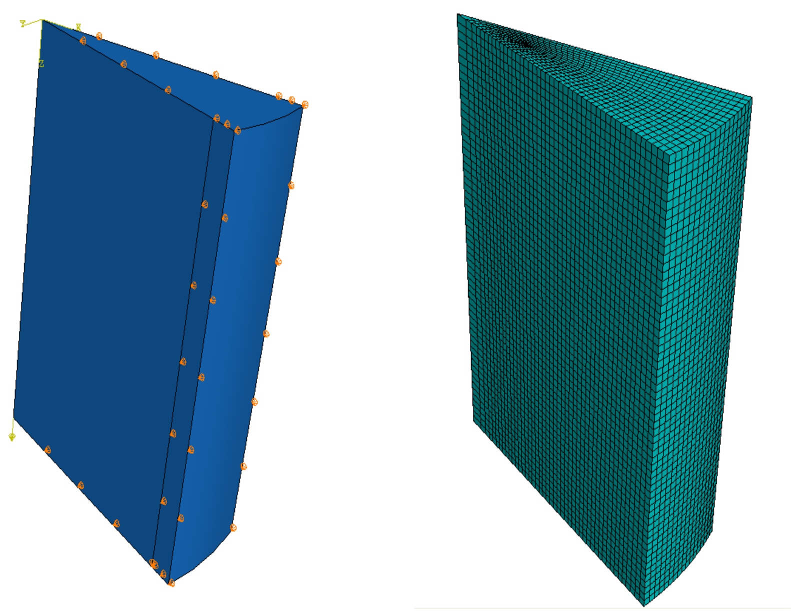

(a) (b)

Figure 5. 3-D test case, a) loads and boundary conditions, b) finite element mesh.

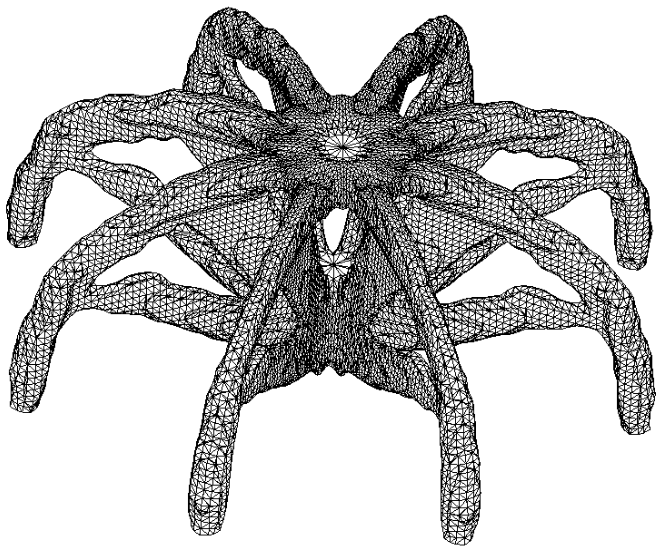

Figure 6. 3-D test case – numerically generated topology.

A second family of 3-D test cases is minimum weight tubular truss structures subjected to combined axial and torsion load. For pure torsion loading, the optimal tubular truss consists of members oriented along spirals (11) at ±45° with the tube axis. For pure axial loading, truss members oriented parallel to the tube direction provide the minimum weight design. For combined loading with axial load *F* and torque *T*, the optimal cylindrical structure layout comprises orthogonal families of helices intersecting the axial direction at angles γ and $(\pi/2-\gamma)$ respectively, where

$$\gamma = \cot^{-1}\left(\left(Fr/T\right)/2\right)/2 \qquad (6)$$

The topology of such a structure is illustrated in Figure 7.

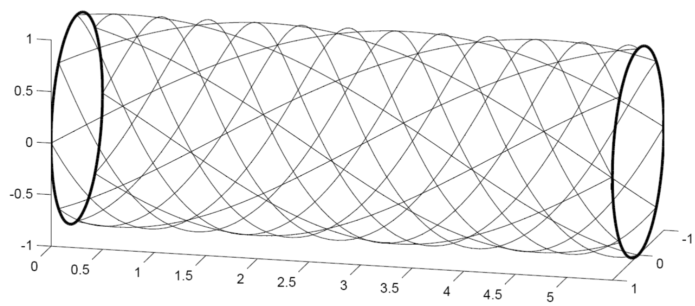

Figure 7. Helical spirals for combined axial and torsion loads (γ=π/6).

For this problem, the design domain is taken to be a thick walled cylinder subjected to concentrated forces at the ends of the cylinder given by f_n in the axial and f_t in the tangential directions. The finite element model along with the optimized results for the case of pure torsion (f_n=0, f_t=1) are shown in Figure 8. This figure shows the domain and boundary conditions, the final density field and an image of the STL model created during post-processing. The STL models for varying combinations of axial and torsion loadings are shown in Figure 9. The helix angle, γ, was estimated from these models and compared to the theoretical optimum given in Equation 6. As shown in Figure 10, the numerical scheme accurately predicts the optimum helix angle for all cases.

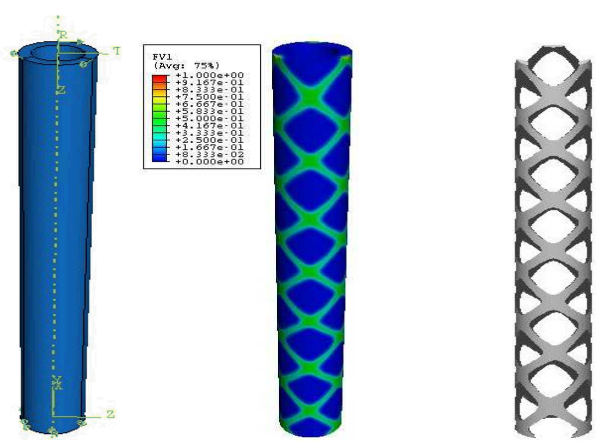

Figure 8. Pure torsion, cylindrical domain – numerically generated topology.

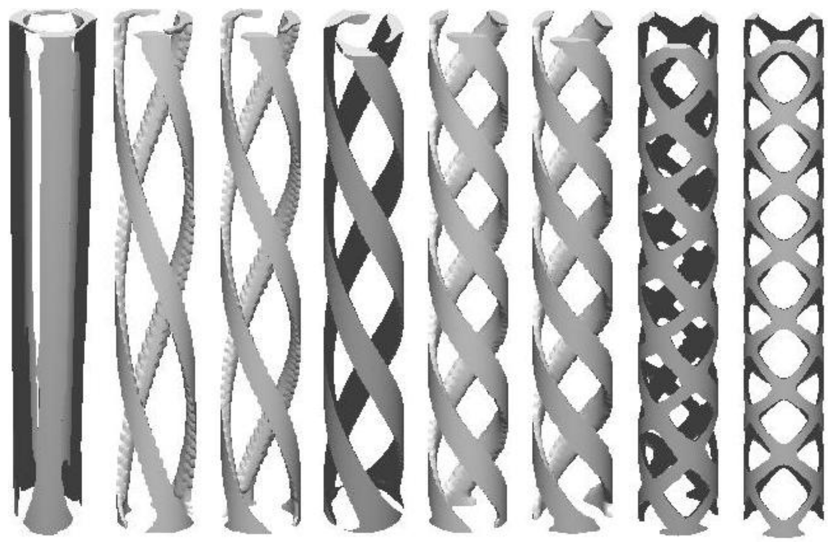

Figure 9. Results for combined axial and torsion loads (f_n/f_t=∞, 3.464, 2.383, 1.678, 0.727, 0.352 and 0)

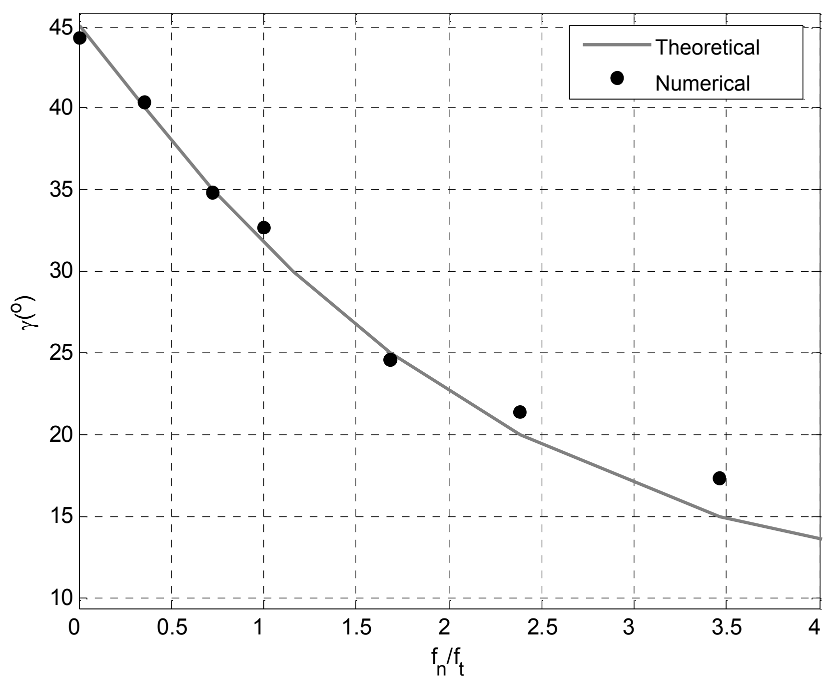

Figure 10. Comparison of theoretical and numerical optimum helix angle, γ.

Another interesting 3-D test case involves pure torsion loading with the design domain taken to be of infinite extent. For modeling purposes, the infinite domain is approximated by a thick wall cylinder (Figure 12) in which the inner and outer diameter extend well beyond the expected minimum weight topology. As shown in Figure 11, circumferential forces are applied along a circular path near the inner diameter of the cylinder. At the opposite end of the cylinder, nodes along the corresponding circular path are constrained such that motion in the axial and circumferential directions is prevented. The minimum weight topology was identified by Michell (8) to consist of loxodromes, or spherical spirals, oriented at ±45° with longitudinal lines as shown in Figure 12. The numerical optimization scheme accurately predicts this topology (see Figure 13). Using the STL file generated by the post-processing code, a physical model was fabricated on an Dimension SST 3-D printer and is shown in Figure 14.

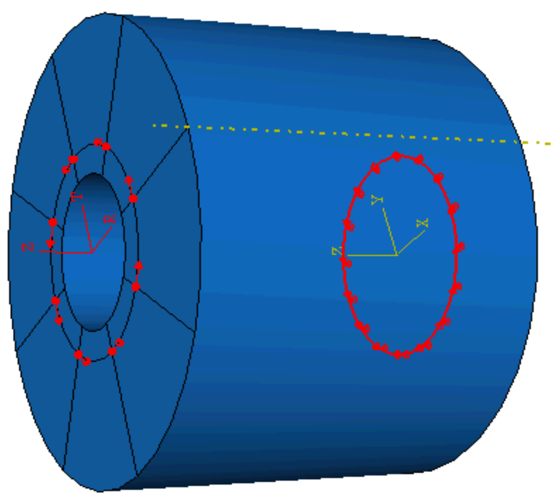

Figure 11. Pure torsion, infinite domain - loads and boundary conditions

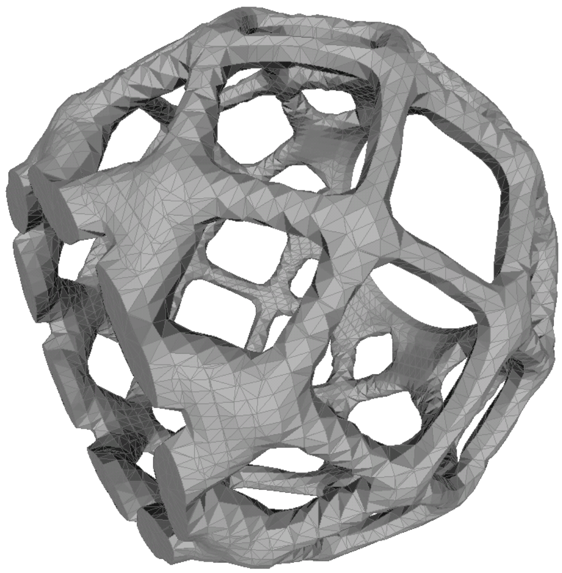

Figure 13. Pure torsion, infinite domain - numerically generated topology.

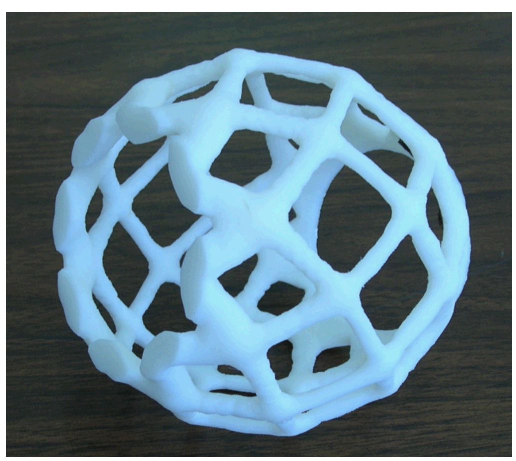

Figure 14. Prototype component manufactured from STL file.

5. Application to Component Design

To illustrate application to an aerospace component design, the numerical optimization scheme was applied to the design of an optical lens assembly shown in Figure 15. The particular component selected for optimization is the housing. The housing is supported through three flexures which are bonded to three mounting brackets. The loads on the mounting bracket consist of six axial forces equally spaced around the perimeter of the lens support region and are associated with contact with a wave spring. For simplicity, details of the support region design are not considered and the optimization is applied to the cylindrical region of the housing.

For this analysis, the mass of the housing was held equal to that of the original design. Hence, the optimized structure (Figure 16) is both stronger and stiffer than the original design. Using Laser Engineered Net Shaping™ (LENS®), a prototype optimized component was manufactured from the STL file as shown in Figure 17.

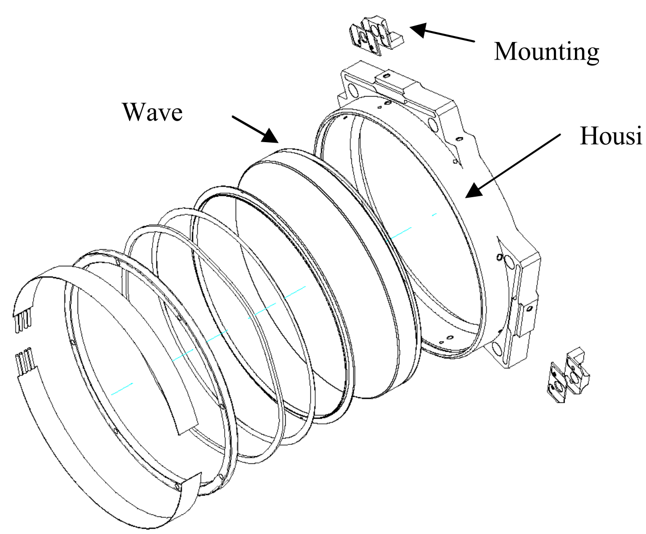

Figure 15. Optical lens assembly.

® Laser Engineered Net Shaping™ and LENS® are registered trademarks of Sandia National Laboratories

Figure 16. Optimized lens housing.

Figure 17. Prototype component manufactured from STL file.

6. Conclusions

A novel finite element topology optimization procedure is presented. This procedure is shown to identify minimum-weight topologies for several 2-D and 3-D problems for which the optimal topology is known from classical theoretical solutions. It is believed that this scheme provides an efficient method for identifying optimal topologies for complex design problems. Since the scheme has been implemented using user subroutines in Abaqus, application to general design problems is simplified due to the robust user interface tools for both problem definition and visualization of final results. Finally, the generation of STL format models of the optimized structure provides visualization and rapid manufacturing capability.

7. References

1. Bendsoe, M. P., and Kikuchi, N., "Generating optimal topologies in structural design using a homogenization method," Computer Methods in Applied Mechanics and Engineering, 71, 197-224, 1988.
2. Bendsoe, M. P. and Sigmund, O., "Topology Optimization," Springer-Verlag, 2004.
3. Xie, Y. M. and Steven, G. P., "A simple evolutionary procedure for structural optimization," Computers and Structures, 49, 885-896, 1993.
4. Xie, Y. M., and Steven, G. P., "Evolutionary structural optimization," Springer, London, 1997.
5. Nair, A., Demircubuk, M., Dewhurst, P. and Taggart, D., "Evolutionary techniques for identifying minimum weight topologies and for the suppression of global instabilities," ABAQUS Users Conference, May 2005.
6. Nair, A., Taggart, D. and Dewhurst, P. "A novel evolutionary topology optimization algorithm," in preparation.
7. Abaqus Analysis User Subroutine Reference Manual, version 6.6, Abaqus, Inc., Providence, RI, 2006.
8. Michell, A. G. M., "Limits of economy of material in frame-structures", Philosophical Magazine, 6, 589-597, 1904.
9. Chan, A. S. L., "The design of Michell optimum structures," Report No. 142, College of Aeronautics, Cranfield UK, December 1960.
10. Lorensen, W. and Cline, H. E., "Marching Cubes: A High Resolution 3D Surface Construction Algorithm", Computer Graphics - Proceedings of SIGGRAPH '87, Vol. 21, No. 4, pp. 163-169, 1987.
11. Dewhurst, P. and Taggart, D. G., "Analysis of minimum weight symmetrical structures for combined axial and torsional loading," in preparation for submission to Structural and Multidisciplinary Optimization, 2008.

8. Acknowledgement

The authors would like to appreciation to Sandia National Laboratories, Albuquerque, New Mexico, for support of this work.